

Structure and mechanical properties of (Mo, Re)Si₂ alloys

T.E. Mitchell *, A. Misra

Center for Materials Science, Los Alamos National Laboratory, Los Alamos, NM 87545, USA

Abstract

Hot hardness tests have been performed on arc-melted (Mo, Re)Si₂ alloys at temperatures from ambient to 1300°C. Re is found to be a potent solution hardening addition to MoSi₂ over the entire temperature range, much more than would be expected from their atomic size mismatch or modulus mismatch. In addition ReSi_{2-x} has about twice the hardness of pure MoSi₂ at all temperatures. This may be related to the structure of ReSi_{2-x} which nominally has the same tetragonal C11_b structure as MoSi₂ but is Si-deficient ($x = 0.25$, i.e. the composition is Re₄Si₇). The Si deficiency is accompanied by some unusual incommensurate periodicities in the structure which themselves give rise to orthorhombic and monoclinic distortions. The resulting microstructure probably explains the high strength of Re₄Si₇ and the potent hardening effect of Re in MoSi₂ may be due to the accompanying Si vacancies. © 1999 Elsevier Science S.A. All rights reserved.

Keywords: Mechanical properties; Alloys; Temperature range

1. Introduction

MoSi₂ single crystals have an unusually rich array of slip systems and most orientations show compression plasticity down to ambient temperatures [1,2]. The available critical resolved shear stress (CRSS) data are shown in Fig. 1. Many of the slip systems are on the close-packed {110} and {013} planes but slip on {0kl} planes with $\langle 100 \rangle$ Burgers vectors is also common. Slip on the {013} plane involves the long $1/2\langle 331 \rangle$ Burgers vector and this even operates at ambient temperatures for crystals compressed along $\langle 100 \rangle$. There are several unusual features arising from Fig. 1:

- All slip systems show yield stress anomalies where the CRSS increases with increasing temperature over a range of temperatures.
- [001] crystals are brittle below 900°C even though the {013} $\langle 331 \rangle$ system is available for this orientation.
- Polycrystalline MoSi₂ remains stubbornly brittle to temperatures well above 1000°C in spite of all the operable slip systems with modest CRSS values at temperatures well below 1000°C in Fig. 1.

Yield stress anomalies are quite common in inter-metallics and have their origin in either extrinsic factors such as the Portevin–Le Chatelier effect, or intrinsic factors such as the nature of the dislocation core [3]. The reason why [001] MoSi₂ and polycrystalline MoSi₂ are brittle in spite of the availability of suitable slip systems is unclear. However, alloying strategies may help overcome the problem.

The difficulty of substitutional alloying of MoSi₂ is that most elements destabilize the tetragonal C11_b structure [4]. For example, modest additions of other disilicide formers such as Nb, Cr and Ti stabilize the hexagonal C40 structure which only deforms on the basal plane and does not have the variety of slip systems exhibited by MoSi₂. The only other disilicides that have the C11_b structure are WSi₂ and, reportedly, ReSi₂; as described below, the latter is not strictly true. Both W and Re can be substituted for Mo in MoSi₂. Since MoGe₂ also has the C11_b structure, it is likely that Ge can be substituted for Si. We have also found that a few percent Al can substitute for Si in MoSi₂ while retaining the C11_b structure, resulting in hardness reduction and possibly improved fracture toughness [5]; larger additions give the less desirable C40 structure [6]. In the present paper we will describe the results of alloying Re to MoSi₂ and also an investigation of the structure and mechanical properties of ReSi_{2-x}.

* Corresponding author. Tel.: +1-505-6670938; fax: +1-505-6652992; e-mail: temitchell@lanl.gov.

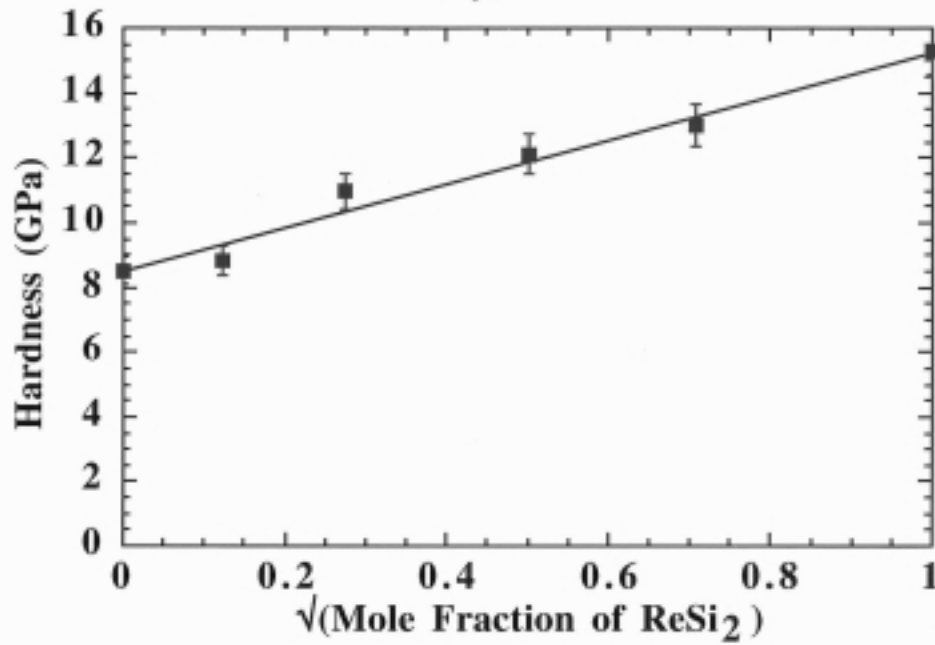
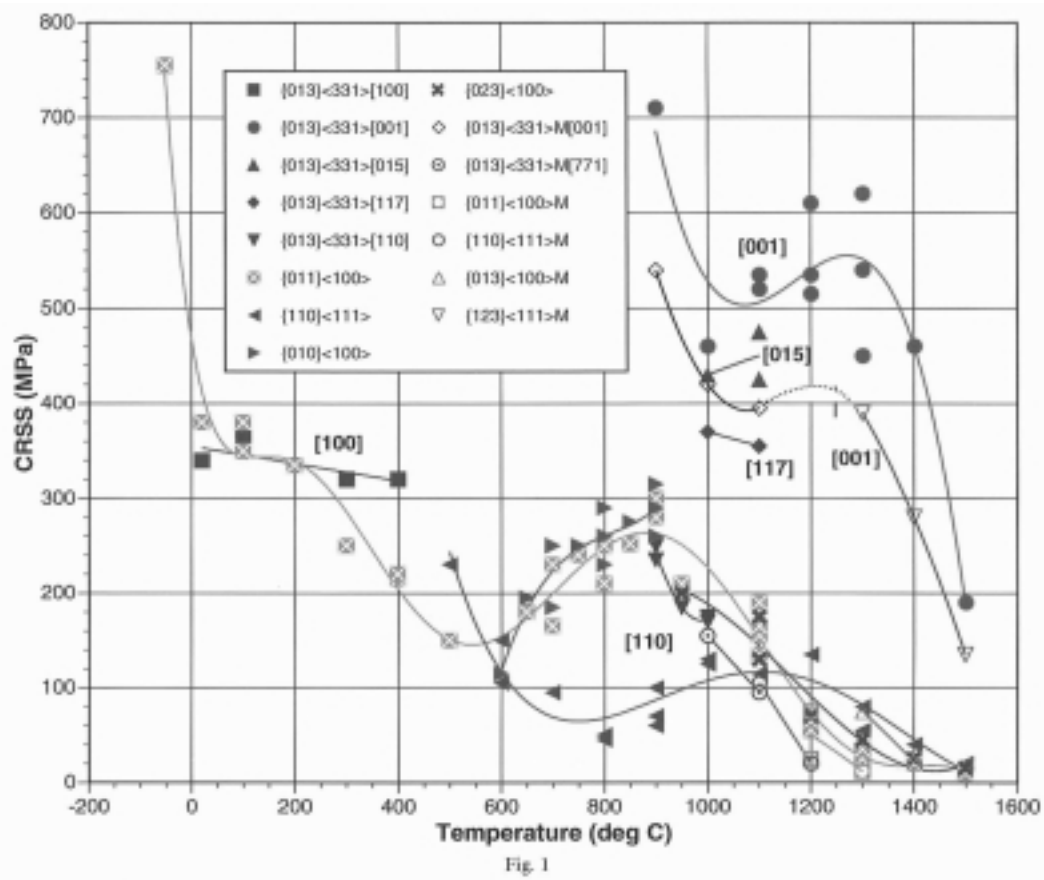


Fig. 1. Plots of CRSS vs. temperature for MoSi_2 deformed in compression along various orientations as shown. Much of the data is from Ito et al. [1]; the data marked with M in the legend are from Maloy et al. [2].

Fig. 6. Room temperature hardness of $(\text{Mo}_{1-x}, \text{Re}_x)\text{Si}_2$ alloys plotted against $x^{1/2}$.

Table 1
Previous studies of the composition and structure of ReSi_{1-x}

Composition	Structure type	Lattice parameters	References
ReSi_2	Tetragonal C11_b	$a = 3.132 \text{ \AA}$, $c = 7.681 \text{ \AA}$	Neshpor and Samsanov, 1964 [13]
$\text{ReSi}_{1.8}$	Tetragonal C11_b	$a = 3.132 \text{ \AA}$, $c = 7.681 \text{ \AA}$	Jorda et al., 1982 [20]
$\text{ReSi}_{1.99}$	Orthorhombic distortion of C11_b	$a = 3.144 \text{ \AA}$, $b = 3.128 \text{ \AA}$, $c = 7.677 \text{ \AA}$	Siegrist et al., 1983 [21]
$\text{ReSi}_{1.75}$	Monoclinic distortion of C11_b	$a = 3.139 \text{ \AA}$, $b = 3.121 \text{ \AA}$, $c = 7.670 \text{ \AA}$, $\beta = 89.87^\circ$	Gottlieb et al., 1995 [7]
$\text{ReSi}_{1.75}$	Incommensurate monoclinic structure based on C11_b	$b/a = 1.006$, $\beta = 89.6^\circ$	Misra et al., 1998 [8]; present study

2. Experimental

(Mo, Re) Si_2 and ReSi_{2-x} alloys were prepared by arc-melting elemental Mo, Re and Si with nominal purities of 99.999% in an argon atmosphere. The buttons were turned over and remelted 5–6 times to ensure homogeneity. Some alloys were also grown into single crystals or large-grained textured polycrystals by the Czochralski technique, using a tri-arc furnace, or by optical float zone melting. Rectangular parallelepipeds with dimensions $5 \times 5 \times 10 \text{ mm}^3$ were cut from the as-grown crystals or arc-melted buttons. The samples were polished with SiC paper to $3 \mu\text{m}$ and finished with $0.05 \mu\text{m}$ colloidal silica. Hardness was determined with a Nikon QM-2 hot hardness tester in vacuum over a range of temperatures from ambient to 1300°C . All hot hardness experiments were performed on polycrystalline materials with $75\text{--}100 \mu\text{m}$ grain size. Thin foils for transmission electron microscopy (TEM) were prepared from some of the undeformed material by ion-milling. TEM was performed on either a Philips CM30 operated at 300 kV or a JEOL JEM3000F for high resolution work.

3. Results and discussion

3.1. Composition and structure of ReSi_{2-x}

Results of previous studies of the composition and structure of ReSi_{2-x} are summarized in Table 1. The most reliable X-ray diffraction study is that of Gottlieb et al. [7] who found the stoichiometry to be $\text{ReSi}_{1.75}$ (or Re_4Si_7) and detected orthorhombic and monoclinic distortions to the C11_b structure, as given in Table 1. Our own study [8] gave the same stoichiometry; attempts to prepare ‘rhenium disilicide’ always resulted in free silicon in the microstructure whereas a composition corresponding to Re_4Si_7 was always single phase. The microstructure of rhenium disilicide has been published elsewhere [8].

As we have reported previously [8], the selected area diffraction patterns (SADP's) observed in Re_4Si_7 are generally in accord with the results of Gottlieb et al. [7]

in that there are small orthorhombic and monoclinic distortions to the underlying C11_b structure, as indicated in Table 1. However, most importantly, the cause of the distortions is a strong incommensurate periodicity of $4.14a$ along the a -axis (hereafter called structure A). Longer period incommensurate structures are also seen along the c -axis but these are less consistent. In addition, in some regions of the same specimen there is a much larger monoclinic distortion corresponding to a shear of 17° along the c -axis; the incommensurate periodicity along the a -axis is retained (hereafter called structure B). Whether A or B occurs probably depends on the local cooling rate. Indeed, we have recently examined specimens that were annealed for 48 h at 1250°C and then furnace cooled. These were found to have a *commensurate structure* in which the diffraction spots of structure B are shifted from the incommensurate $4.14a$ periodicity to a commensurate $4a$ periodicity. The difference between the three structures is illustrated in Fig. 2 where $[010]$ SADP's are shown for each structure. The diffraction patterns are distinctly different but the underlying C11_b structure is evident in all of them.

A variety of twinned microstructures is observed. In fact the diffraction patterns from structures B and C in Fig. 2(a,b), respectively, result from twinned variants with the twin plane perpendicular to the c -axis. (We have previously called the twinned microstructure in B a ‘chevron’ structure due to the interference fringes observed). Even the A structure has (001) twins due to the small monoclinic distortion, as illustrated in Fig. 3. In addition, structure A has (110) twin boundaries separating domains where the incommensurate periodicity is along the a or b axes of the C11_b structure. This suggests that Re_4Si_7 has the C11_b structure at high temperatures and then forms the incommensurate structure A during cooling where the incommensuration can occur along the equivalent a and b axes of the C11_b structure. The reason for the different structures that form must be the difficulty of accommodating such a high density of structural Si vacancies ($\sim 14\%$) in the C11_b structure. A possible sequence of transformation events is as follows:

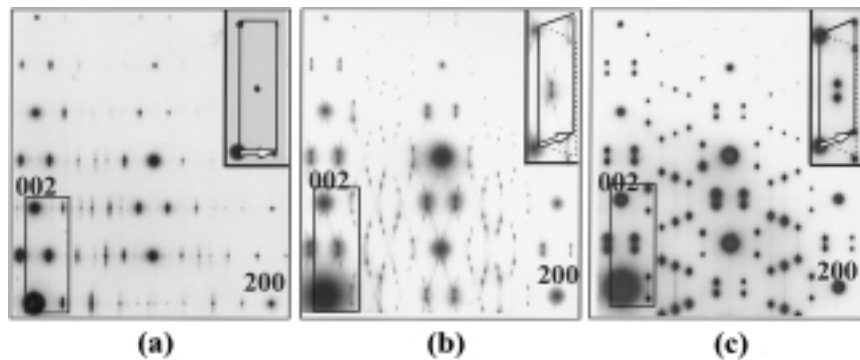


Fig. 2. [010] SADP's from Re_4Si_7 : (a) structure A, weakly monoclinic with incommensurate diffraction spots along a axis; (b) structure B, distinctly monoclinic with incommensurate periodicity; and (c) structure C (after annealing at 1250°C), also monoclinic but with extra commensurate reflections. The boxed regions are enlarged in the insets for each of the three diffraction patterns showing the vector defining the incommensurate or commensurate periodicity.

- At high temperatures the Si structural vacancies in Re_4Si_7 are distributed randomly and the structure is tetragonal C11_b .
- During normal cooling, the Si vacancies have insufficient time to order in a commensurate structure and the incommensurate structure A is formed instead.
- For some conditions of time and temperature, possibly a slower cooling rate, structure A transforms to structure B by a shear of 17° along the c -axis.
- Prolonged annealing at intermediate temperatures allows sufficient time for the Si vacancies to order and form the commensurate structure C.

Besides Re_4Si_7 , the 'disilicides' of Mn and Tc (all group VIIB elements) also have stoichiometries of Mn_4Si_7 and Tc_4Si_7 , respectively, [9]. In fact, for disilicides of Mn, at least four different structures were discerned by high-resolution electron microscopy: Mn_4Si_7 , $\text{Mn}_{11}\text{Si}_{19}$, $\text{Mn}_{15}\text{Si}_{26}$ and $\text{Mn}_{27}\text{Si}_{47}$, all in the narrow range of Si to Mn ratio of 1.75 to 1.72 [10]. The tetragonal structures of the defect silicides of Mn and

Tc have been interpreted as Nowotny 'chimney-ladder' phases derived from the orthorhombic TiSi_2 structure-type [9]. In these structures, the Mn atoms form the 'chimneys' within which the Si atoms are arranged in a 'ladder' [9,10]. Incommensurate structures result when the Mn sub-cell parameter is not commensurate with the Si sub-cell parameter. A similar Nowotny phase type of structure may be possible for Re_4Si_7 as well where the different structures observed may result from small changes in composition, with the exception that the host structure is MoSi_2 and not TiSi_2 .

3.2. Mechanical properties of Re_4Si_7 and $(\text{Mo}, \text{Re})\text{Si}_2$ alloys

Hardness values as a function of temperature from ambient to 1300°C are shown in Fig. 4 for pure MoSi_2 , Re_4Si_7 and a $(\text{Mo}_{0.925}, \text{Re}_{0.075})\text{Si}_2$ alloy. The MoSi_2 data are for both hot-pressed and arc-melted material [11,12]; the values are essentially the same with a hint of

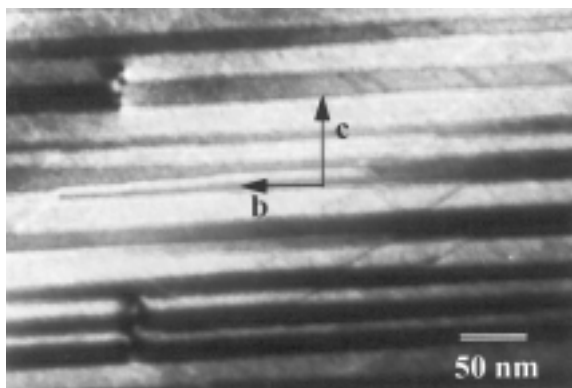


Fig. 3. The set of twins in structure A due to the monoclinic distortion. The twin boundaries are parallel to the (001) plane (referred to the underlying C11_b structure).

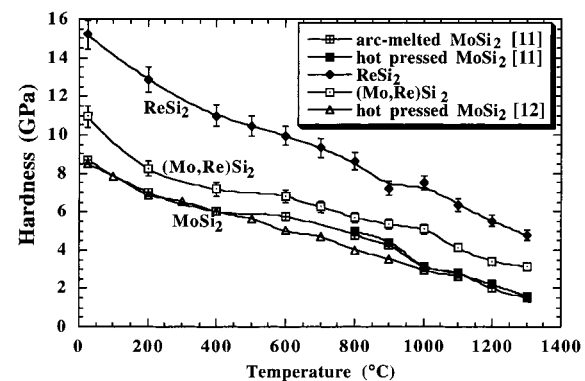


Fig. 4. Hardness vs. temperature curves for MoSi_2 , Re_4Si_7 and a $(\text{Mo}_{1-x}, \text{Re}_x)\text{Si}_2$ alloy with $x = 0.075$. The data for MoSi_2 are from Gibala et al. [11] and Maloy et al. [12].

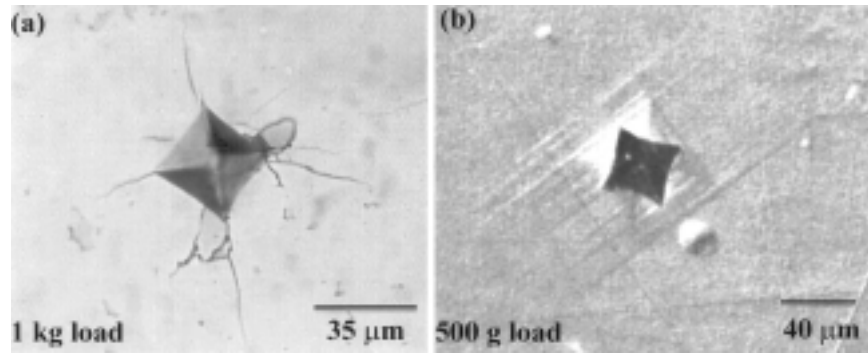


Fig. 5. Light micrographs of indentations in a $(\text{Mo}_{0.925}, \text{Re}_{0.075})\text{Si}_2$ alloy indented at: (a) 25°C; and (b) 800°C. Note the cracks in (a) and the slip lines in (b).

the stress anomalies that are observed in single crystals between 400 and 1000°C (Fig. 1). Fig. 4 shows that Re_4Si_7 is much harder than MoSi_2 over the entire temperature range—almost twice as hard at room temperature and more than three times as hard at 1300°C. The ternary alloy has intermediate hardness values at all temperatures and the results show that Re is a potent solution hardening addition. Substitution of 7.5% Re for Mo increases the hardness of MoSi_2 by 30% at room temperature and 100% at 1300°C. Typical hardness indents for $(\text{Mo}_{0.925}, \text{Re}_{0.075})\text{Si}_2$ alloy are shown in Fig. 5. Prominent cracking behavior is observed at temperatures less than 600°C, such as shown in Fig. 5(a), while slip activity is discerned around indents at higher temperatures, such as shown in Fig. 5(b); occasional cracks are observed around hardness indents in the temperature range 600–1000°C and none at higher temperatures. The increase of hardness with increasing Re substitution is continuous, as shown in Fig. 6 where hardness of $(\text{Mo}_{1-x}, \text{Re}_x)\text{Si}_2$ is plotted against $x^{1/2}$ at ambient temperature. The significance of the straight line relationship is unknown but it implies that the initial hardening rate from Re substitution is high and then gradually decreases. Hardness of $(\text{Mo}, \text{Re})\text{Si}_2$ alloys has also been studied by Neshpor and Samsanov [13], Davidson and Bose [14] and Harada et al. [15]; all observed strong solution hardening and the latter in particular showed that Re was more effective than any of their other alloying additions (Cr, Zr, Nb, Ta and W).

The high hardness of Re_4Si_7 is not surprising in view of its complex microstructure, including the dense twin arrays such as the ones shown in Fig. 3. Typical dislocation structures produced under a hardness indent at 1200°C are shown in Fig. 7, including the results of a $\mathbf{g} \cdot \mathbf{b}$ analysis. Dislocations with Burgers vectors $1/2\langle 111 \rangle$, $\langle 100 \rangle$ and $\langle 110 \rangle$ are observed where the indexing of both \mathbf{g} and \mathbf{b} is with respect to the underlying tetragonal C11_b sublattice and the incommensurate

structure is ignored. Possibly the structure is C11_b at the temperature of deformation so that the observed Burgers vectors are the same as in MoSi_2 , except for the absence of $1/2\langle 331 \rangle$ dislocations. The various twins and incommensurate structures are not observable for the beam direction in Fig. 7 (near $[110]$). However, it should be appreciated that all of the dislocations are partial dislocations with respect to the actual structure.

The hardening rate due to Re substitution can be calculated from Figs. 4 and 6 to be

$$\begin{aligned} \frac{\Delta\sigma}{\Delta x} &= \frac{\mu}{18} \text{ at } 25^\circ\text{C} \\ &= \frac{\mu}{27} \text{ at } 1300^\circ\text{C} \end{aligned}$$

where the yield stress has been taken to be a third of the hardness and μ is the shear modulus. Such high hardening rates would qualify Re as a rapid hardener whereas, in view of the fact that the size mismatch is modest (the Goldschmidt radii for Mo and Re are 1.40 and 1.38 Å, respectively) and the modulus mismatch is also modest (μ values for MoSi_2 and Re_4Si_7 are 191 and 149 GPa, respectively, [16]), Re would be expected to be a moderate substitutional alloy hardener [17]. Early work suggested that MoSi_2 and ReSi_2 form a complete range of solid solutions [13]. In view of the present work and that of Gottlieb et al. [7], this cannot be correct and, at some value of x in $(\text{Mo}_{1-x}, \text{Re}_x)\text{Si}_2$, there must be a phase change from the C11_b structure to the distorted structures. It is also likely that Si vacancies accompany the substitution of Re for Mo in order to reduce the electron concentration and bring the Fermi energy down from its position in the antibonding states toward the energy gap. This would result in the observed increase in electrical resistivity and decrease in hole conductivity as x increases. Furthermore it is likely that the Re substitutionals and Si vacancies would attract each other both elastically and

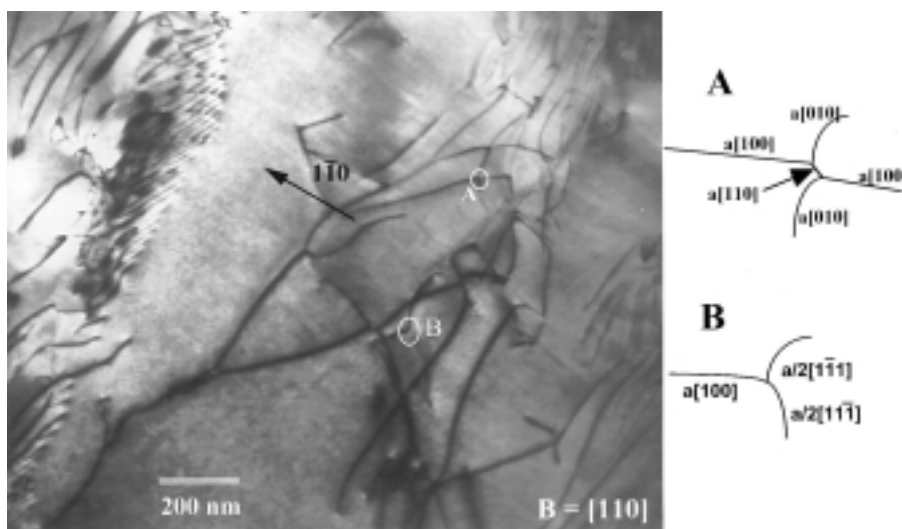


Fig. 7. Bright field TEM image of dislocations produced under a hardness indent at 1200°C. The beam direction is close to $[110]$ and $g = 110$, referred to the underlying $C11_b$ structure. Results of a $g \cdot b$ analysis for regions A and B are shown to the right.

electrically. The resulting defect complexes would then be more potent hardeners than isolated Re substitutionals and could explain the observed rapid solution hardening.

The key to understanding why the stoichiometry is Re_4Si_7 and not $ReSi_2$ is that it is a narrow band gap semiconductor. This is only possible if it has an even number of electrons, which is true of Re_4Si_7 but not $ReSi_2$. In fact electronic structure calculations have been performed on ' $ReSi_2$ ' [18,19] and the resulting density of states curve is given in Fig. 8. Note that the Fermi level falls in the band containing anti-bonding

states. Assuming rigid band behavior and insensitivity of the calculations to structural distortions (both questionable assumptions), changing the stoichiometry to Re_4Si_7 should reduce the electron concentration and move the Fermi level into the energy gap between the bonding and anti-bonding states. This should reduce the lattice energy and thereby explain the structural Si vacancies and the resulting structural distortions.

4. Conclusions

1. Rhenium disilicide has a stoichiometry of Re_4Si_7 , giving it an even number of electrons and explaining why it is a narrow band gap semiconductor.
2. Re_4Si_7 has three distinct structures which are distorted forms of the tetragonal $C11_b$ structure, two incommensurate and one commensurate; they correspond to different ways that the Si vacancies are arranged.
3. The three crystal structures of Re_4Si_7 are all probably monoclinic and twinned microstructures result from the transformations.
4. The hardness of Re_4Si_7 is 2–3 times greater than $MoSi_2$ over the entire temperature range from ambient to 1300°C; this is interpreted in terms of its complex twinned and incommensurate microstructure.
5. Re is a potent solution hardener in $(Mo_{1-x}Re_x)Si_2$ alloys. The hardening rate is greater than expected from the usual size and modulus misfit and is explained in terms of the association of Re substitutionals and Si vacancies into defect complexes.

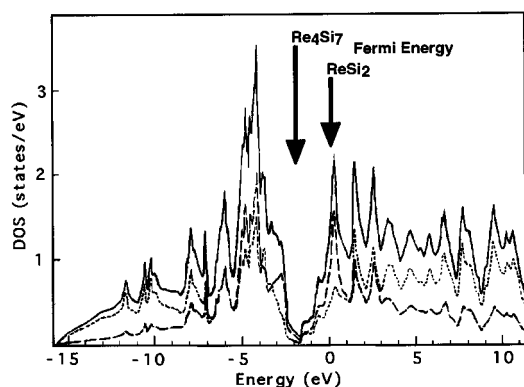


Fig. 8. Density of states curves for ' $ReSi_2$ ' calculated by Itoh [18]. The solid, broken and dotted lines indicate the total, Si-projected and Re-projected densities of states, respectively. The calculated Fermi energy of $ReSi_2$ is indicated; the Fermi energy of Re_4Si_7 is suggested to occur within the gap between the bonding and anti-bonding states.

Acknowledgements

This research was performed under the auspices of the US Department of Energy, Office of Basic Energy Sciences. We thank F. Chu, K.J. McClellan and P. Peralta for assistance with arc-melting, crystal growth and hot-hardness testing.

References

- [1] K. Ito, M. Moriwaki, T. Nakamoto, H. Inui, M. Yamaguchi, *Mater. Sci. Eng. A* 233 (1997) 33.
- [2] S.A. Maloy, T.E. Mitchell, A.H. Heuer, *Acta Metall. Mater.* 43 (1995) 657.
- [3] D. Caillard, A. Couret, in: F.R.N. Nabarro, M.S. Duesbery (Eds.), *Dislocations in Solids*, Elsevier, Amsterdam, 1996, p. 69.
- [4] W.J. Boettinger, J.H. Perepezko, P.S. Frankwicz, *Mater. Sci. Eng. A* 155 (1992) 33.
- [5] P. Peralta, S.A. Maloy, F. Chu, J.J. Petrovic, T.E. Mitchell, *Scr. Mater.* 37 (1997) 1599.
- [6] H. Inui, M. Moriwaki, K. Ito, M. Yamaguchi, *Phil. Mag. A* 77 (1998) 375.
- [7] U. Gottlieb, B. Lambertandron, F. Nava, M. Affronte, O. Laborde, A. Rouault, R. Madar, *J. Appl. Phys.* 78 (1995) 3902.
- [8] A. Misra, F. Chu, T.E. Mitchell, *Phil. Mag. A*, (1999) (in press).
- [9] H. Nowotny, in: L. Eyring, M. O'Keefe (Eds.), *The Chemistry of Extended Defects in Non-Metallic Solids*, North-Holland, Amsterdam, 1970, p. 223.
- [10] H.Q. Ye, S. Amelinckx, *J. Solid State Chem.* 61 (1986) 8.
- [11] R. Gibala, A.K. Ghosh, D.C. Vanaken, D.J. Srolovitz, A. Basu, H. Chang, D.P. Mason, W. Yang, *Mater. Sci. Eng. A* 155 (1992) 147.
- [12] S.A. Maloy, A.H. Heuer, J.J. Lewandowski, J.J. Petrovic, *J. Am. Ceram. Soc.* 74 (1991) 2704.
- [13] V.S. Neshpor, G.V. Samsanov, *Fiz. Metal. Metalloved.* 18 (1964) 187.
- [14] D.L. Davidson, A. Bose, *Mat. Res. Soc. Symp. Proc.* 322 (1994) 431.
- [15] Y. Harada, Y. Funato, M. Morinaga, A. Ito, Y. Sugita, *Jpn. Inst. Metals* 58 (1994) 1239.
- [16] A. Misra, F. Chu, T.E. Mitchell, *Scr. Mater.* 38 (1998) 917.
- [17] R.L. Fleischer, *Acta Metall.* 11 (1963) 203.
- [18] S. Itoh, *Mater. Sci. Eng. B* 6 (1990) 37.
- [19] B.K. Bhattacharaya, D.M. Bylander, L. Kleinmann, *Phys. Rev. B* 33 (1986) 3947.
- [20] J.L. Jorda, M. Ishikawa, J. Muller, *J. Less-Common Met.* 85 (1982) 27.
- [21] T. Siegrist, F. Hullinger, G. Travaglini, *J. Less-Common Met.* 92 (1983) 119.